Life Sciences 287 (2021) 120123

Contents lists available at ScienceDirect

Life Sciences

journal homepage: www.elsevier.com/locate/lifescie

idiopathic pulmonary fibrosis

Eirini Filidou [a], Leonidas Kandilogiannakis [a], Gesthimani Tarapatzi [a], Colin Su [b], Emilie Ng Foong Po [b], Vasilis Paspaliaris [b], George Kolios [a,*]

[a] Lab of Pharmacology, Faculty of Medicine, Democritus University of Thrace, Alexandroupolis, Greece
[b] Tithon Biotech Inc, San Diego, CA 92127, USA

ARTICLE INFO

Keywords:
Mesenchymal stem cell conditioned medium
Mesenchymal stem cells
Idiopathic pulmonary fibrosis
Bleomycin model
Fibrosis

ABSTRACT

Idiopathic pulmonary fibrosis is a chronic, progressive parenchymal lung disease that results in fibrogenesis and the conditioned medium from adipose-derived mesenchymal stem cells (CM-ADSCs) has been shown to be efficacious in pulmonary fibrosis animal models. The aim of the present study is to evaluate the effect of CM-ADSCs on lung inflammation and fibrosis in a Bleomycin (BLM)-induced pulmonary fibrosis model. CM-ADSCs safety and toxicity were evaluated in Sprague Dawley rats and no adverse effects were observed. Six-week-old female C57BL/6J mice were employed in the BLM-induced pulmonary fibrosis model and were divided into four groups: Group 1 (Sham): animals were kept without BLM and treatment, Group 2 (Control): BLM with vehicle DMEM, Group 3: 10 μg/kg CM-ADSCs and Group 4: 100 μg/kg CM-ADSCs. Body weight, fibrosis and inflammation histological analyses, mRNA and protein pro-inflammatory cytokine, and total hydroxyproline content calculation were performed in all groups upon sacrifice. The 100 μg/kg CM-ADSCs showed a significant increase in mean body weight compared to Controls. CM-ADSCs doses resulted in the amelioration of fibrosis, as seen by Masson's Trichrome-staining, Ashcroft scoring, and Sirius red-staining. Compared to Controls, inflammation was also significantly reduced in CM-ADSCs-treated mice, with reduced F4/80 macrophage antigen staining, TNF-α mRNA and IL-6 and IL-10 protein levels. Total hydroxyproline content was found significantly reduced in both groups of CM-ADSCs-treated mice. Overall, our study shows that the CM-ADSCs is safe and efficient against pulmonary fibrosis, as it significantly reduced inflammation and fibrosis, with the larger dose of 100 μg/kg CM-ADSCs being the most efficient one.

1. Introduction

Idiopathic pulmonary fibrosis (IPF) is a chronic, progressive parenchymal lung disease that results in fibrosis [37]. The clinical course of the disease is unpredictable and can be characterized by a progressive course of several years or by a rapid deterioration leading to death in a few months with a median survival of 3–5 years following diagnosis [26]. The aetiology of IPF is not understood and a number of risk factors, such as smoking and gastroesophageal reflux disease, have been suggested to be associated with the development of the disease [28]. The morbidity and mortality rate of IPF is extremely high and most of the current anti-fibrotic therapies may slightly slow the progression of the disease, but it has been shown to be ineffective in preventing or reversing its rapid progression [37].

Mesenchymal Stem Cells (MSCs), also known as mesenchymal stromal cells, have immunomodulatory, differentiative and self-renewing properties, and are commonly used in regenerative medicine [40]. Plasticity and tropism are the main classifications of their features with the first to indicate their capacity to differentiate into different components to respond to a specific stimulus and the latter their ability to

Abbreviations: IPF, Idiopathic Pulmonary Fibrosis; MSCs, Mesenchymal Stem Cells; CM, Conditioned Medium; CM-ADSCs, Conditioned Medium from Adipose-Derived Mesenchymal Stem Cells; hTERT, human Telomerase Reverse Transcriptase; PFA, Paraformaldehyde; BSA, Bovine Serum Albumin; WBC, White Blood Cell; DAT, Direct Antiglobulin Test; BLM, Bleomycin; NOAEL, No Observed Adverse Effect Level.

* Corresponding author at: Laboratory of Pharmacology, Faculty of Medicine, Democritus University of Thrace, Dragana, Alexandroupolis 68100, Greece.
E-mail address: gkolios@med.duth.gr (G. Kolios).

https://doi.org/10.1016/j.lfs.2021.120123
Received 24 September 2021; Received in revised form 31 October 2021; Accepted 2 November 2021
Available online 6 November 2021

move to diseased or damaged cells and tissues [6,29,39]. MSCs contain a unique set of features that make them attractive and suitable for their therapeutic potential in inflammatory illnesses and regenerative medicine [40].

Human mesenchymal stem cells have been shown to down-regulate inflammatory responses and to produce anti-inflammatory cytokines and growth factors to promote tissue repair [42]. Conditioned medium (CM) derived from such cells has been shown to be safe and efficacious in animal models of pulmonary fibrosis [31]. Administration of conditioned medium from adipose-derived mesenchymal stem cells (CM-ADSCs) has been shown to be safe and efficacious in both animal models and human clinical trials of pulmonary fibrosis and other chronic obstructive pulmonary diseases [5,6,31]. CM-ADSCs is the sterile collection of ex-vivo conditioned medium, secreted by adipose-derived mesenchymal stem cell lines in vitro, and containing immunoregulatory cytokines and growth factors [24,48]. Many studies have shown that the administration of mesenchymal stem cell-derived conditioned medium in acute doses in humans is safe and well-tolerated [9,18,25]. Based on its tolerability and safety profile, CM-ADSCs is a promising alternative to live mesenchymal stem cell therapy in diseases with an unmet need such as IPF [31,40]. The aim of the present study is to evaluate the effect of CM-ADSCs on lung inflammation and fibrosis in a BLM-induced pulmonary fibrosis model.

2. Materials and methods

1. Adipose-derived mesenchymal stem cell isolation and immortalization

Adipose-derived mesenchymal stem cells were isolated as previously described [4], from subcutaneous adipose tissue, obtained during outpatient tumescence liposuction under local anesthesia from a 35-year-old healthy female, who was informed and agreed to participate in this study by giving her written consent. All principles outlined in the Declaration of Helsinki for all human experimental investigations were followed. Next, the adipose-derived stem cells were immortalized by employing a previously described method [4]; transduction performed with the human telomerase reverse transcriptase (hTERT) gene in combination with lentiviral gene SV-40.

2. Characterization of immortalized human adipose-derived stem cells

The immortalized human adipose-derived stem cells were characterized by immunofluorescence as previously described [14]. Briefly, cells were first fixed in 4% paraformaldehyde (PFA; Sigma-Aldrich, St. Louis, Missouri, United States) for 40 min at 4 °C, then membrane permeabilization was achieved by a 15-min incubation with 0.1% Triton-X (Sigma-Aldrich, St. Louis, Missouri, United States) and blocking was performed using 5% bovine serum albumin (BSA; Sigma-Aldrich, St. Louis, Missouri, United States) for 1 h. Primary antibodies (Novus Biologicals, Littleton, Colorado, USA) against the mesenchymal markers of CD90, CD105 and vimentin and the hematopoietic marker of CD34 were added and left overnight at 4 °C, and secondary fluorochrome-conjugated antibodies (Novus Biologicals, Littleton, Colorado, USA) were added the following day and left for 2 h. Finally, nuclei were stained with DAPI (Sigma-Aldrich, St. Louis, Missouri, United States) and samples were observed under a fluorescent microscope (Leica DM2000, Leica Microsystems GmbH, Germany). As seen in Supplementary Fig. 1, the immortalized human adipose-derived stem cells were positive for CD90, CD105 and vimentin and negative for CD34.

3. Conditioned medium preparation

Conditioned medium from immortalized human adipose-derived stem cells (CM-ADSCs) was provided by Tithon Inc. San Diego, CA, USA, which was collected and processed as follows. A total of 1 × 105 cells were plated in T-25 flasks in medium containing DMEM (Gibco; Thermo Fisher Scientific, Waltham, Massachusetts, USA), high glucose (4.5 g/L) with 2% L-glutamine, 10% FBS (Gibco; Thermo Fisher Scientific, Waltham, Massachusetts, USA) and gentamycin 1% (Gibco; Thermo Fisher Scientific, Waltham, Massachusetts, USA), at 37 °C, 5% CO_2. Upon the cells becoming confluent, the medium was changed to FBS-free medium. Supernatants were collected every 72 h and fresh FBS- free medium was added. Cell supernatants were harvested and centri- fuged at 2500 rpm for 10 min at 4 °C and filtered through a 0.45 μm filter (Merck-Millipore, Burlington, Massachusetts, USA) to remove cell debris and cryopreserved at 80 °C until use. Total protein was measured, as previously described [20], using the Bio-Rad protein microassay, which is based on Bradford's dye-binding procedure.

4. Acute toxicity study

1. Animals and toxicity study design

Acute toxicity study of CM-ADSCs was investigated in Sprague Dawley rats, since it is widely accepted and recognized by international guidelines as an appropriate experimental model for this type of acute toxicity study [34]. The CM-ADSCs was administered subcutaneously as a single dose to a group of 10 rats (5/sex) at a dose of 1 mg/kg (equivalent to approximately 10 mg dose in humans). A control group of 10 rats (5/sex) received the vehicle (DMEM media and 0.1% benzyl alcohol in water) at the same volume. Body weights were determined immediately before the administration of CM-ADSCs and weekly thereafter (Days 1, 8 and 15). All animals were observed daily for signs of toxicity over the 14-day experimental period. At the end of the experimental period, on Day 15, all surviving animals were sacrificed, and gross necropsy was performed.

2. Organ weight evaluation

Following animal sacrifice and dissection, the liver, kidneys, adrenals, gonads, and spleen were harvested from each animal and immediately weighed wet.

3. Histopathological analysis

After organ weighing, representative samples of each animal's organ were collected, fixed in 10% formalin, processed, embedded in paraffin, and cut into 5 μm thicknesses. Hematoxylin and eosin staining was performed according to standard immunostaining protocols. Histopathological analysis on the tissue samples of all animals was carried out by a veterinary pathologist.

4. Immune cell quantities and functionality

Prior to animal sacrifice, blood samples were collected from all animals, and host immune cell quantities and functionality were determined in obtained plasma samples. Specifically, for immune cell quantities, total white blood cell (WBC) count was investigated and for immune cell functionality, WBC subgroups (granulocytes, monocytes and lymphocytes) quantities were measured using an automated hematology analyzer, Sysmex XS (Sysmex Corporation, Kobe, Japan).

5. Alloantibody evaluation

In order to examine any alloantibody formation, Direct Antiglobulin Test (DAT) was performed. Polyspecific antisera that would detect either IgG and/or complement was added to each animal's plasma serum and since, no positive results occurred, no monospecific IgG or complement was tested. Possible agglutinating antibodies on red blood cells was evaluated by mixing each animal's blood samples with antisera solutions, samples were then incubated at room temperature and finally examined microscopically for agglutination.

5. Idiopathic pulmonary fibrosis animal model

1. Animals

Six-week-old female C57BL/6J mice were obtained from Japan SMC, Inc. (Japan). Prior to the induction of idiopathic pulmonary fibrosis, all animals were kept on a normal diet (CE-2; Lot# E2040-A6, E2050-PL, CLEA Japan) and under controlled conditions, as previously described [7]. The following guidelines were applied to all animals included in this study: 1) Act on Welfare and Management of Animals (Ministry of the Environment, Act No. 105 of October 1, 1973); 2) Standards Relating to the Care and Management of Laboratory Animals and Relief of Pain (Notice No.88 of the Ministry of the Environment, April 28, 2006) 3) Guidelines for Proper Conduct of Animal Experiments (Science Council of Japan, June 1, 2006). The animals were maintained in an SPF facility under controlled conditions of temperature (23 ± 3 °C), humidity (50 ± 20%), lighting (12-h artificial light and dark cycles; light from 8: 00 to 20:00) and air exchange.

2.5.2. Induction of BLM-induced pulmonary fibrosis model

Bleomycin (BLM)-induced pulmonary fibrosis was conducted by SMC Laboratories, Inc. Japan (Study Number SLMP019-2007-06). At Day 0 and 6, pulmonary fibrosis was induced to mice by a single dose of 3.0 mg/kg bleomycin hydrochloride (Lot# 391870, BLM, Nippon Kayaku, Japan) diluted in saline, via intratracheal administration using Microsprayer® (Penn-Century, USA), as previously described [21]. The BLM administrations took place on two separate days. Mice were divided into two groups by random sampling before BLM administration. Twelve normal mice were intratracheally administered saline instead of BLM and served as the Sham group. Thirty-six mice were intratracheally administered BLM and were randomized into 3 groups of 12 mice based on the body weight changes on the day before the start of treatment at Day 7. One group did not receive treatment and the rest were intravenously administered, through the tail vain, escalated doses of CM-ADSCs three times a week from Day 7 to 20. Total protein of CM-ADSCs was measured and CM-ADSCs was then diluted in DMEM (Gibco, Thermo Fisher Scientific, Waltham, Massachusetts, United States) in order to prepare the two studied doses; 10 μg/kg and 100 μg/kg. Groups: Group 1 (Sham): Twelve normal animals were kept without BLM and treatment and sacrificed at Day 21. Group 2 (Control): BLM with vehicle DMEM. Group 3: 10 μg/kg CM-ADSCs. Group 4: 100 μg/kg CM-ADSCs. During the experimental period, daily observations on the survival, clinical signs and behaviour of mice and measurements of body weights were performed, as previously described [7]. If an animal lost >40% of its body weight, compared to Day 0, and/or if it showed a moribundity sign, such as a prone position, the animal was euthanized ahead of study termination and its samples were not collected. Mice were intravenously administered various doses of CM-ADSCs, three times a week, from Day 7 to 20. The viability, clinical signs (lethargy, twitching, laboured breathing), and behaviour were monitored daily. Body weight was recorded daily from Day 0. Dosing volume was adjusted based on the latest body weight. After each administration, animals were under careful observation for any significant toxicity, moribundity and mortality sign, as previously described [7]. The animals were sacrificed at Day 21 by exsanguination through the abdominal aorta under a mixture of medetomidine (Nippon Zenyaku Kogyo Co., Ltd., Japan), midazolam (Sandoz K.K., Japan) and butorphanol (Meiji Seika Pharma Co., Ltd., Japan) anesthesia. The time of the dosing and termination were recorded.

2.5.3. BALF collection and analyses

BALF samples from all groups were collected by flushing the lung via the trachea with 0.8 mL of sterile PBS at sacrifice under a mixture of medetomidine (0.75 mg/kg), midazolam (4 mg/kg) and butorphanol (5 mg/kg) anesthesia. The BALF was centrifuged at 3000 x*g* for 5 min at 4 °C and the supernatant was collected and stored at 80 °C for biochemistry. Samples of BALF from mice were examined for the expression of the cytokine levels of IL-6 and IL-10 using Mouse IL-6 Quantikine ELISA Kit and Mouse IL-10 Quantikine ELISA Kit, respectively (R&D Systems, Inc., USA).

4. Total RNA extraction and DNase treatment

Around 10 mg of lung tissue was mechanically homogenized in 500 μl Nucleozol (MACHEREY-NAGEL, Düren, Germany) and total RNA was extracted according to the manufacturer's instructions. In short, H_2O was added to each sample, following incubation and a 15 min centrifugation at 12.000 *g*. Supernatants were then incubated with isopropanol and centrifuged for 10 min at 12.000 g in order to precipitate the RNA. The RNA pellet was washed twice with 75% ethanol and reconstituted with H_2O. Total RNA concentration was measured using Quawell Q5000 UV–Vis Spectometer (Quawell, San Jose, California, United States). Any DNA contaminations were removed using Recombinant DNase I (TaKaRa, Kusatsu, Shiga, Japan).

5. cDNA synthesis and real-time PCR

200 ng of the DNAse treated RNA was reverse transcripted using the PrimeScript 1st strand cDNA Synthesis Kit (TaKaRa, Kusatsu, Shiga, Japan) according to the manufacturer's instructions. Following cDNA synthesis, 25 ng cDNA was then amplified with qRT-PCR using Sybr Green (Kapa Biosystems, Wilmington, USA) and 200nM of gene-specific primers for TGF-β1, TNF-α and IL-1β (Table 1) in SaCycler-96 RUO (Sacace Biotechnologies, Como, Italy).

A two-step amplification protocol was performed for all studied genes and the gene expression of each studied gene was normalized against GAPDH gene expression in the same sample using the 2-ΔΔCt method.

6. Measurement of lung hydroxyproline

Hydroxyproline expression was evaluated and measured in frozen left lung samples by an acid hydrolysis method, as previously described [7]. Briefly, HCl was first added to the lung samples in order to be acid-hydrolyzed, followed by the addition of neutralizing NaOH containing 10 mg/mL activated carbon. Next, samples were mixed with AC buffer (2.2 M acetic acid/0.48 M citric acid), centrifuged and the supernatant was collected. Trans-4-hydroxy-L-proline (Sigma-Aldrich Co. LLC., USA) was used for the construction of a standard curve of known hydroxyproline concentrations. Chloramine T solution (NACALAI TESQUE, INC., Japan) was then added to the lung samples and the known hydroxyproline concentrations, followed by 25 min incubation at room temperature. Color development was achieved by the addition of Ehrlich's solution to both samples and the known hydroxyproline concentrations. The optical density of each supernatant was measured at 560 nm and the concentrations of hydroxyproline were calculated from the hydroxyproline standard curve.

7. Histological analyses

Right lung tissues prefixed in 10% neutral buffered formalin were embedded in paraffin and sectioned at 4 μm. For Masson's Trichrome staining, the sections were deparaffinized and rehydrated, followed by re-fixation with Bouin's solution (Sigma-Aldrich). The sections were stained in Weigert's iron Hematoxylin working solution (Sigma- Aldrich), Biebrich scarlet-Acid fuchsin solution (Sigma-Aldrich), Phosphotungstic/phosphomolybdic Acid solution, Aniline blue solution and 1% Acetic Acid solution (Sigma-Aldrich). Lung fibrosis area was quantitated as previously described [7]. Briefly, a digital camera (DFC295; Leica, Germany) at 100-fold magnification was employed for capturing various random bright field images of Masson's Trichrome-stained sections, and the subpleural regions in 20 fields/mouse were evaluated according to the criteria for grading lung fibrosis [3]. Ashcroft score was calculated for each photographed image, and the average value of 20 fields/mouse of view was taken as the individual's Ashcroft score.

To visualize collagen deposition, the lung sections were deparaffinized and hydrophilized and then treated with 0.03% picro-Sirius red

Table 1
Primer sequences used in real time PCR expression experiments.

Gene	Forward	Reverse	Reference
GapdH	AACTTTGGCATTGTGGAAGG	GGATGCAGGGATGATGTTCT	[12]
TGF-β1	CCCCACTGATACGCCTGAGT	AGCCCTGTATTCCGTCTCCTT	[16]
TNF-α	ATCCGCGACGTGGAACTG	ACCGCCTGGAGTTCTGGAA	[36]
IL-1β	AATGCCACCTTTTGACAGTGAT	TGCTGCGAGATTTGAAGCTG	[17]

solution. The stained sections were dehydrated and cleared with 70–100% alcohol series and xylene, then sealed with Entellan® rapid mounting medium (Merck, Germany) and used for observation. Similar to the Masson's Trichrome-staining quantification, Sirius red positive staining areas of fibrosis was also quantified as previously described [7]. A digital camera (DFC295) at 100-fold magnification was utilized for capturing various bright field images of Sirius red-stained sections, and the positive areas in 5 fields/section were measured using ImageJ software (National Institute of Health, USA).

For immunohistochemistry, the sections were deparaffinized and hydrophilized. Endogenous peroxidase activity was blocked using 0.3% H_2O_2, and antigen retrieval was performed using antigen retrieval solution H (citrate buffer). After washing with PBS, lung sections were treated with PBS containing Tween 20 (PBST), followed by incubation with Block Ace (DS Pharma Biomedical Co. Ltd., Japan). The sections were incubated with anti-F4/80 antibody overnight and after incubation with secondary antibody, enzyme-substrate reactions were performed using 3, 3′-diaminobenzidine/H_2O_2 solution (Nichirei Bioscience Inc., Japan). Lung sections were fixed with 1% glutaraldehyde solution and then coloured using chromogenic substrate (Simple Stain DAB, Nichirei Bioscience Inc., Japan) and hematoxylin solution. Quantification of F4/80-positive areas was performed as previously described [7]; a digital camera (DFC295) at 100-fold magnification was employed for capturing various and random bright field images of F4/80-immunostained sections, and the F4/80-positive area in 5 fields/section were measured using ImageJ software (National Institute of Health, USA).

2.6. Statistical analysis

Statistical analyses were performed using Prism Software 9 (GraphPad Software, USA). For survival analysis, the Kaplan-Meier analysis with the Log-Rank test was performed. For other data, statistical analyses were performed using Bonferroni Multiple Comparison Test. p values <0.05 were considered statistically significant. Results were expressed as mean ± SD.

3. Results

1. Animal toxicity study

Upon CM-ADSCs administration, the body weight of the female and male rats was in the range of 193–210 and 252–278 g, respectively. No mortalities occurred during the study. No abnormal clinical signs were seen during the 14-days observation period. Treated and vehicle control groups showed similar body weight gains over the 14-day observation period (Table 2).

Table 2
Mean Body Weights (g). Results are expressed as mean ± SD. In both males and females, Group 1 $N = 5$ and Group 2 $N = 5$.

Parameter	Males		Females	
	Group 1 Vehicle control	Group 2 1 mg/kg	Group 1 Vehicle control	Group 2 1 mg/kg
Day 1	260 ± 6.3	262 ± 9.9	212 ± 6.7	203 ± 8.2
Day 8	311 ± 10.9	312 ± 16.1	229 ± 8.7	223 ± 13.1
Day 15	348 ± 17.4	350 ± 20.7	248 ± 12.2	242 ± 15.2

No significant macroscopic differences in any organs were observed during gross necropsy in any animals. Organ weights when expressed as a percentage of body weight were not affected by the treatment (Table 3).

No effects on host immune cell quantities or immune system functionality were observed. There was no evidence of alloantibody formation (data not shown). Under the conditions of the study, for the CM-ADSCs, the no observed adverse effect level (NOAEL) was determined to be greater than 1 mg/kg (193–278 g) and the relevant NOAEL in mice could be translated to approximately 2 mg/kg, based on publicly available conversion guidelines [15,33].

3.2. The CM-ADSCs administration results in full body weight recovery in BLM-induced mice

The body weight of animals was expressed as percentage of body weight change from baseline (Day 0). Mean body weight changes of the Control group were significantly lower than that of the Sham group from Day 16 to 21, reaching 93.73% ±16.13 for the Control and 107.7% ±2.42 for the Sham group at Day 21. Regarding the effect of CM-ADSCs, the administrated dose of both 10 μg/kg and 100 μg/kg resulted in statistically significant full body weight recovery at Day 21, when compared to Control; 10 μg/kg: 107.3% ±2.71, $p < 0.01$ and 100 μg/kg: 105.8% ±4.63, $p < 0.05$ (Fig. 1).

Regarding animal survival, there were no significant differences in survival rate between the CM-ADSCs Control group and the other groups (Fig. 2).

3.3. Histological analyses reveal reduced fibrosis and inflammation in CM-ADSCs-treated mice

Regarding our histological analyses, Masson's Trichrome-staining revealed no fibrotic findings in the Sham group, as expected (Fig. 3A), and intense ones in the Control group (Fig. 3B).

The administration of either CM-ADSCs dose resulted in the amelioration of fibrosis (Fig. 3C 10 μg/kg and Fig. 3D 100 μg/kg), with the higher dose to be more efficient as it almost reversed fibrosis (Fig. 3D). In order to quantitatively grade lung fibrosis, we calculated the Ashcroft score in each mice group. The Control group showed a statistically significant increase in Ashcroft score compared with the Sham group (Control: 2.9 ± 1.16, $p < 0.0001$; Fig. 3E). The administration of CM-ADSCs resulted in a dose-dependent decrease in the Ashcroft score, with the dose of 100 μg/kg to be statistically significant, as it reduced more than half the Ashcroft score when compared to Control (100 μg/kg: 1.16 ± 0.61, $p < 0.05$; Fig. 3E).

Table 3
Percentage Organ Weights (%). Results are expressed as mean ± SD. In both males and females, Group 1 $N = 5$ and Group 2 $N = 5$.

Parameter	Males		Females	
	Group 1 Vehicle control	Group 2 1 mg/kg	Group 1 Vehicle control	Group 2 mg/kg
Liver	5.10 ± 0.51	4.70 ± 0.36	4.75 ± 0.17	4.72 ± 0.31
Kidneys	0.81 ± 0.05	0.81 ± 0.06	0.78 ± 0.04	0.85 ± 0.07
Adrenals	0.015 ± 0.004	0.013 ± 0.002	0.04 ± 0.01	0.03 ± 0.01
Gonads	0.83 ± 0.09	0.97 ± 0.13	0.04 ± 0.01	0.05 ± 0.02
Spleen	0.21 ± 0.03	0.22 ± 0.02	0.21 ± 0.03	0.23 ± 0.04

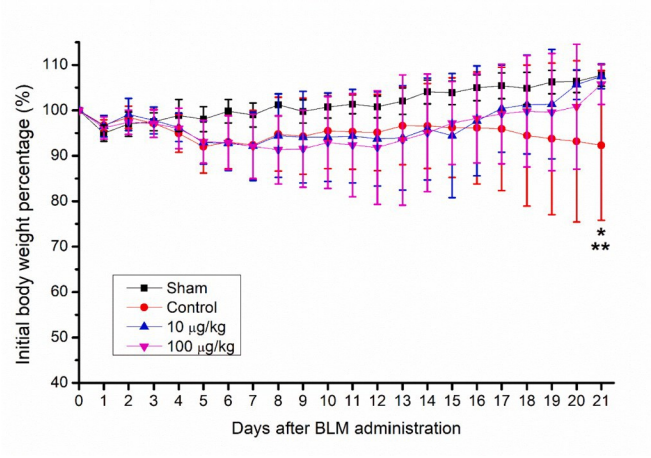

Fig. 1. The effect of CM-ADSCs administrative doses on body weight recovery. Body weight percentages were calculated by setting the baseline to initial body weight at Day 0. Sham group $N = 12$, Control group $N = 11$, 10 μg/kg $N = 8$ and 100 μg/kg $N = 9$. Statistical analysis was performed using Bonferroni Multiple Comparison Test.

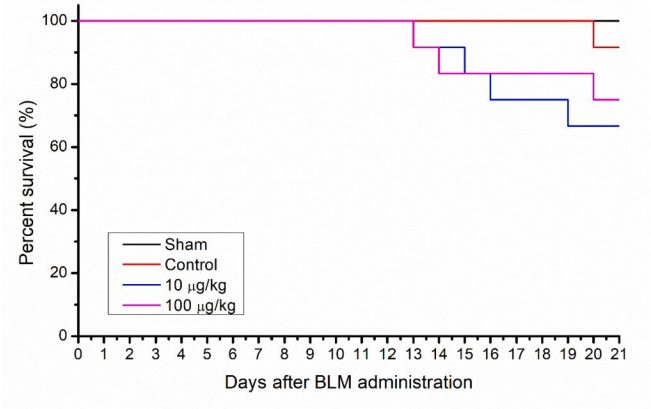

Fig. 2. Survival percentage rate of mice included in the study. All mice survived in the Sham group. Among the other groups, only one from the Control, four from the 10 μg/kg CM-ADSCs and three from the 100 μg/kg CM-ADSCs group did not survive, with no statistically significant differences among them. Sham group $N = 12$, Control group $N = 11$, 10 μg/kg $N = 8$ and 100 μg/kg $N = 9$. Statistical analysis was performed using the Kaplan-Meier analysis with the Log-Rank test.

In accordance with the aforementioned histological analyses are the results from Sirius red-staining. As seen in Fig. 4, the Sham group was negatively stained for Sirius red (Fig. 4A), while the Control group was presented with intense staining, suggesting established fibrosis (Fig. 4B). Regarding the groups that received CM-ADSCs, the fibrosis area in the 10 μg/kg dose group tended to decrease compared with the Control group (Fig. 4C) and interestingly, the fibrosis area of the 100 μg/kg group was significantly decreased to a point close to the Sham group (Fig. 4D). Further quantitative analysis of Sirius red positive staining areas revealed that the staining percentage of the Control group was at 2.62 ± 1.29, $p < 0.0001$ compared to the Sham group (Fig. 4E), while Fig. 4E).

Regarding inflammation, we first performed F4/80 macrophage staining and found no inflammation in the Sham group (Fig. 5A) and intense positive macrophage staining in the Control group (Fig. 5B).

The administration of 10 μg/kg CM-ADSCs, although statistically not significant, showed a tendency for reduced F4/80 macrophage staining compared to the Control group, (Fig. 5C), while the administration of 100 μg/kg CM-ADSCs did indeed have a greater effect, as it statistical significantly reduced inflammation (Fig. 5D). Specifically, further analysis of the F4/80 positive staining areas revealed that the 100 μg/kg CM-ADSCs dose resulted in statistically significant 1.07 ± 0.23, $p < 0.01$ positive staining area percentage, compared to the Control group, which was at 2.71 ± 1.17 (Fig. 5E).

3.4. The administration of CM-ADSCs results in the downregulation of mRNA and protein pro-inflammatory expression levels

In order to further assess the effect of CM-ADSCs in lung fibrosis, we examined the mRNA expression of TGF-β1, TNF-α, and IL-1β in lung tissues. The Sham group mice had limited mRNA levels of TGF-β1, TNF-α and IL-1β, while Control group mice had increased expression of TNF-α mRNAs (6.67-fold ±2.37, $p < 0.0001$; Fig. 6A) and TGF-β1 (3.24-fold ±1.95, $p < 0.05$; Fig. 6B).

Regarding the treatment with the CM-ADSCs, the TNF-α mRNA expression was statistical significantly downregulated in a dose-dependent way (10 μg/kg: 1.64-fold ±1.17, $p < 0.01$; 100 μg/kg: 1.13-fold ±0.86, $p < 0.0001$; Fig. 6A), and so did TGF-β1 mRNA expression, although not statistical significantly (Fig. 6B). No significant differences in the mRNA expression of IL-1β were found in any animal group (Fig. 6C).

Having analysed the mRNA expression levels of the aforementioned cytokines, we proceeded to their protein quantification in BALF samples. Although we found changes in the mRNA expression levels of TNF-α, no statistically significant changes were found in its protein expression levels (Data not shown). Nonetheless, we did find significant protein expression changes in IL-6 and IL-10 production. Regarding IL-6, the Control group had a statistically significant increase of IL-6, reaching 84.01 pg/ml ±42.35, $p < 0.0001$, compared to the Sham group (Fig. 7A). When BLM-induced mice received the CM-ADSCs, IL-6 protein production was found decreased in a dose-dependent way compared to the Control group, with the 100 μg/kg dose to significantly reduce its production (6.48 pg/ml ±6.23, $p < 0.01$; Fig. 7A). Similar results were found regarding the IL-10 protein expression in BALF samples. The Control group mice had a statistically increased IL-10 protein production in comparison to the Sham group (3.11 pg/ml ±1.5, $p < 0.0001$; Fig. 7B), while the administration of the 100 μg/kg CM-ADSCs dose completely diminished its production (Fig. 7B).

3.5. Both CM-ADSCs doses significantly reduce total lung hydroxyproline content

Finally, we investigated the total hydroxyproline content in mice lung tissues and as expected, it was found increased in the Control group compared with the Sham group mice (66.4 μg ±16.3, $p < 0.001$; Fig. 8), suggesting again established fibrosis. Interestingly, both CM-ADSCs doses resulted in significant decreased hydroxyproline production, compared to the Control group (10 μg/kg: 49.42 μg ±11.29, $p < 0.05$ and 100 μg/kg: 44.64 μg ±4.84, $p < 0.01$; Fig. 8) verifying again that CM-ADSCs treatment can indeed reverse fibrosis.

4. Discussion

In the present study, we demonstrated that adipose-derived mesenchymal stem cell- conditioned medium ameliorated bleomycin-induced lung fibrosis among the mice that survived the treatment. Specifically, a significant increase in mean body weight on the day of sacrifice compared with the bleomycin control group and significantly decreased fibrotic and inflammatory lung markers were observed. CM-ADSCs treatment also significantly decreased, in a dose-dependent manner,

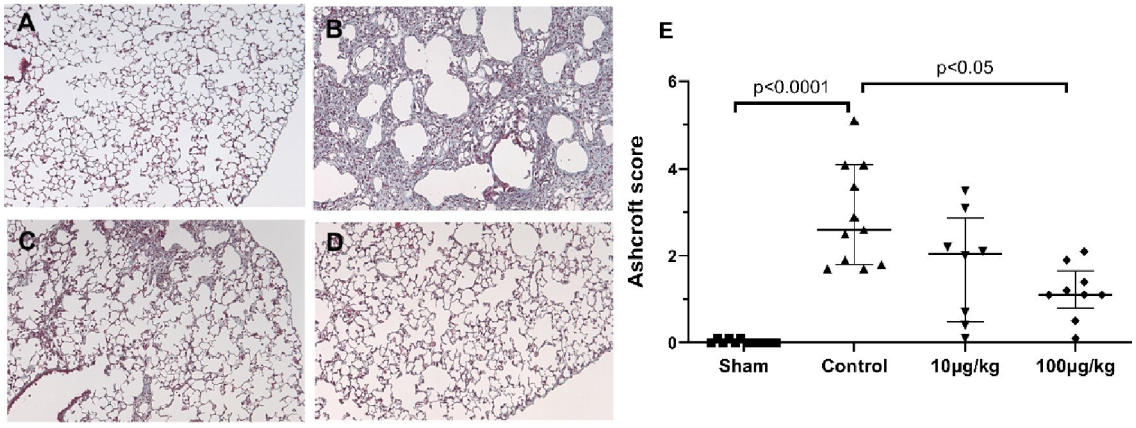

Fig. 3. Masson's Trichrome-staining and Ashcroft scoring. Lung sections treated with Masson's Trichrome-staining of Sham group (A), Control group (B), 10 μg/kg CM-ADSCs (C) and 100 μg/kg CM-ADSCs (D) groups. Magnification was set at 100-fold. Ashcroft score (E) was calculated for each photographed image, and the average value of 20 fields/mouse of view was taken as the individual's Ashcroft score. Sham group $N = 12$, Control group $N = 11$, 10 μg/kg $N = 8$ and 100 μg/kg $N = 9$. Statistical analysis was performed using Bonferroni Multiple Comparison Test.

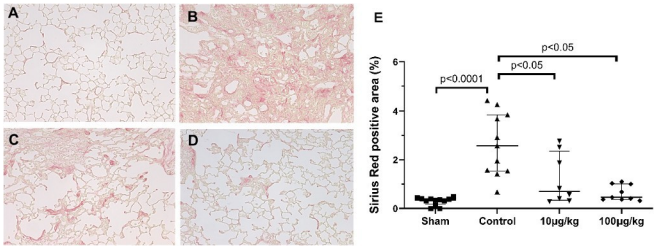

Fig. 4. Sirius red histological staining of lung sections. Lung sections of Sham group (A), Control group (B), 10 μg/kg CM-ADSCs (C) and 100 μg/kg CM-ADSCs (D) groups were stained with Sirius red. Magnification was set at 100-fold. For quantitative analysis of fibrosis area, the positive areas in 5 fields/section were measured using ImageJ software (E). Sham group $N = 12$, Control group $N = 11$, 10 μg/kg $N = 8$ and 100 μg/kg $N = 9$. Statistical analysis was performed using Bonferroni Multiple Comparison Test. (For interpretation of the references to color in this figure legend, the reader is referred to the web version of this article.)

mRNA expression and protein production of proinflammatory cytokines, lung hydroxyproline content, and the fibrotic score, as assessed with the Masson's Trichrome-staining, Ashcroft scoring and Sirius red-staining, compared with the bleomycin Control group. CM-ADSCs treatment began 7 days after BM induction, suggesting that although lung fibrosis was already established when treatment was initiated, the highest dose of CM-ADSCs administration managed to reverse it. Our results are in accordance with several studies that have shown prevention or amelioration of the fibrotic process in various tissues, including lung fibrosis with administration of conditioned medium derived from mesenchymal cells. A recent meta-analysis showed that treatment with mesenchymal stem cell-derived conditioned medium improved pulmonary fibrosis, reducing collagen deposition and inhibiting the production of inflammatory chemokines [2]. Intravenous injection of CM and

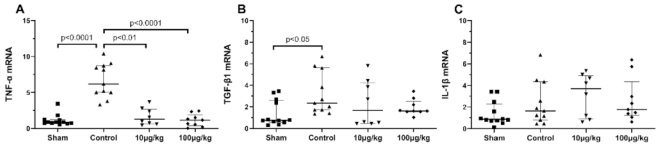

Fig. 6. mRNA expression levels of TNF-α, TGF-β1 and IL-1β. The mRNA levels of TNF-α (A), TGF-β1 (B) and IL-1β (C) were measured in the Sham group and the Control group, 10 μg/kg CM-ADSCs and 100 μg/kg CM-ADSCs groups using qRT-PCR. Sham group $N = 12$, Control group $N = 11$, 10 μg/kg $N = 8$ and 100 μg/kg $N = 9$. Gene expression of each studied gene was normalized against

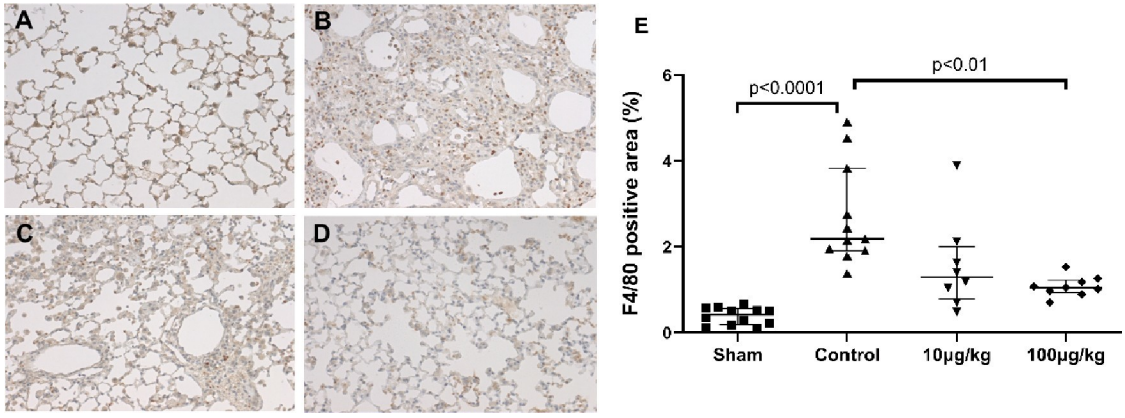

Fig. 5. F4/80 macrophage staining of lung sections. Lung sections of Sham group (A), Control group (B), 10 μg/kg CM-ADSCs (C) and 100 μg/kg CM-ADSCs (D) groups were stained against the F4/80 macrophage antigen. Magnification was set at 100-fold. For quantitative analysis of F4/80-positive area, F4/80-positive area in 5 fields/section were measured using ImageJ software (E). Sham group $N = 12$, Control group $N = 11$, 10 μg/kg $N = 8$ and 100 μg/kg $N = 9$. Statistical analysis was performed using Bonferroni Multiple Comparison Test.

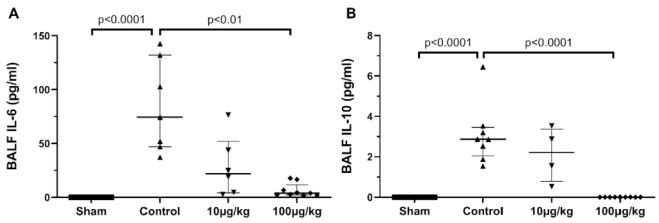

Fig. 7. IL-6 and IL-10 protein expression levels found in BALF samples. The protein levels of IL-6 (A) and IL-10 (B) were measured in the Sham group and the Control group, 10 μg/kg CM-ADSCs and 100 μg/kg CM-ADSCs groups using ELISA immunoassays. Units used in both IL-6 and IL-10 were pg/ml. For IL-6, Sham group $N = 10$, Control group $N = 7$, 10 μg/kg $N = 6$ and 100 μg/kg $N = 9$. For IL-10, Sham group $N = 10$, Control group $N = 8$, 10 μg/kg $N = 4$ and 100 μg/kg $N = 9$. Statistical analysis was performed using Bonferroni Multiple Comparison Test.

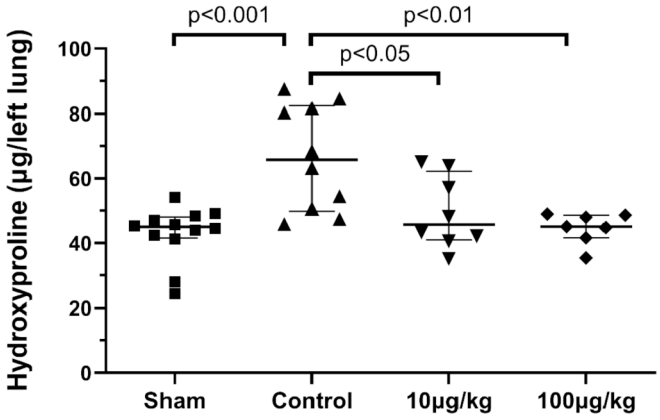

Fig. 8. Total hydroxyproline content found in lung tissues. The total hydroxyproline content was measured in the Sham group, Control group, 10 μg/kg CM-ADSCs and 100 μg/kg CM-ADSCs groups. Units used in hydroxyproline were μg/left lung. Sham group $N = 12$, Control group $N = 10$, 10 μg/kg $N = 8$ and 100 μg/kg $N = 7$. Statistical analysis was performed using Bonferroni Multiple Comparison Test.

MSCs in a rat model with bleomycin-induced pulmonary fibrosis was found to have an immunomodulatory effect, regulating the imbalance between collagen I- and collagen V-mediated IL-17 immune responses and improving fibrosis [13].

In our study, acute toxicity of a single subcutaneous administration of 1 mg/kg of CM-ADSCs in Sprague Dawley rats, showed no adverse effects. Similarly, previous experimental studies performed with live human mesenchymal stem cells or conditioned medium demonstrated that they are safe for therapeutic use [32,42,43,46,49]. However, chronic toxicity, genotoxicity and carcinogenicity studies, as well as animal reproduction and developmental studies have yet to be conducted with conditioned medium.

Initially, scientists attributed MSCs' healing effects to the cells' ability to migrate to the injured cells and areas of inflammation, differentiate into specialized types of cells, and engraft to the damaged tissues [11,27,44]. However, recent scientific studies indicate that the treatment efficacy of transplanted MSCs is not only attributed to their physical proximity to the diseased or damaged cells, [35] but also to their paracrine properties of the large amounts of anti-apoptotic and anti-inflammatory cytokines, growth factor proteins, and microvesicles, such as exosomes, they secrete [8,22]. Thus, MSCs conditioned medium contains the entirety of their secretome, such as distinct exosomes, anti-inflammatory agents like interleukin 1 receptor antagonist and anti-apoptotic agents, such as (IL-6) and insulin growth promoters [1,47]. Therefore, their paracrine properties could enhance anti-inflammatory and angiogenic activity, to decrease collagen deposition and, via the production of matrix metalloproteinases, to exert a fibrinolytic activity reducing the extracellular matrix [30]. These soluble mediators of ADSCs constitute the secretome, which is a complex group of released molecules from the stem cells that carry out additional biological responsibilities, such as apoptosis, cell growth, differentiation, replication, angiogenesis, adhesion, and signaling [41]. The secretome is thought to directly mediate communication between cells or induce the surrounding cells to produce bioactive factors. In sum, the secretome is the main product that carries out different biological functions that make it possible to treat various illnesses, including pulmonary fibrosis. Since the CM contains all the paracrine signaling factors that facilitates tissue and cell repair and regeneration, MSC-CM containing this secretome should have the same therapeutic properties, acting as cell-free substitutes, without limiting the therapeutic efficacy of cell-therapy in treating pathological illnesses [23]. In this study, it was shown that CM-ADSCs ameliorated fibrosis and inflammation in BLM-treated mice, and downregulated various fibrotic and pro-inflammatory factors, suggesting that the ADSCs- secreted soluble mediators present in the CM exert the therapeutic effects observed.

In this study, we also observed that the IL-10 protein production, although unaltered by the 10 μg/kg dose, was significantly reduced by the higher dose of 100 μg/kg. Although CM-ADSCs is thought to exert anti-inflammatory properties, this finding indicates that the secretome's soluble factors may act in a dose-dependent way and when administrated in a high dose, IL-10's expression balance is disturbed. How et al. observed that the CM of induced pluripotent stem cells (iPSCs), among other pro-inflammatory cytokines, it also downregulated the expression of IL-10 [19]. In another study, administration of bone marrow-derived MSCs resulted in a significant decrease of IL-10 and increase of TNF-α [45]. On the other hand, both Dalouchi et al. and Shao et al. showed that the administration of CM in two different disease models resulted in the enhancement of IL-10 production [10,38]. These results clearly indicate that the administrated CM dose plays a significant role in regulating the host's anti-inflammatory responses and that more studies are needed in order to fully comprehend the mechanisms by which the CM exerts its effects.

5. Conclusion

In conclusion, we showed that acute administration of CM-ADSCs, exerts no adverse effects and has the ability to ameliorate lung fibrosis and inflammation. Up until now, most studies on lung fibrosis have been focused on the beneficial effects of administrating ADSCs, while only a few have examined the therapeutic potential of their CM. The results of this study provide significant evidence that CM-ADSCs has therapeutic potential in treating pulmonary fibrosis, a disease with high morbidity and mortality rate in humans and without current successful anti-fibrotic therapies. Future experimental investigation on CM is needed in order to add to its safety profile i.e., further chronic toxicity, genotoxicity, and carcinogenicity studies, and to elucidate the molecular mechanisms of its therapeutic action.

Supplementary data to this article can be found online at https://doi.org/10.1016/j.lfs.2021.120123.

Data availability

The data used to support the findings of this study are available from the corresponding author upon request.

Funding

No funding information to declare.

CRediT authorship contribution statement

Eirini Filidou: Investigation, Formal analysis, Visualization, Writing –original draft. **Leonidas Kandilogiannakis:** Investigation, Formal analysis, Writing – original draft. **Gesthimani Tarapatzi:** Investigation. **Colin Su:** Investigation. **Emilie Ng Foong Po:** Investigation. **Vasilis Paspaliaris:** Conceptualization, Writing – review & editing, Supervision. **George Kolios:** Conceptualization, Writing – review & editing, Supervision.

Declaration of competing interest

The authors declare that they have no known competing financial interests or personal relationships that could have appeared to influence the work reported in this paper.

References

1 S.C. Abreu, D.J. Weiss, P.R. Rocco, Extracellular vesicles derived from mesenchymal stromal cells: a therapeutic option in respiratory diseases? Stem Cell Res Ther 7 (2016) 53.
2 K.M. Ali, F.H.R. Fattah, S.H. Omar, M.I.M. Gubari, M. Yousefifard, M. Hosseini, Mesenchymal stromal cells derived conditioned medium in pulmonary fibrosis: a systematic review and meta-analysis, Arch. Iran. Med. 23 (2020) 870–879.
3 T. Ashcroft, J.M. Simpson, V. Timbrell, Simple method of estimating severity of pulmonary fibrosis on a numerical scale, J. Clin. Pathol. 41 (1988) 467–470.
4 L. Balducci, A. Blasi, M. Saldarelli, A. Soleti, A. Pessina, A. Bonomi, et al., Immortalization of human adipose-derived stromal cells: production of cell lines with high growth rate, mesenchymal marker expression and capability to secrete high levels of angiogenic factors, Stem Cell Res. Ther. 5 (2014) 63.
5 E. Bari, I. Ferrarotti, M.L. Torre, A.G. Corsico, S. Perteghella, Mesenchymal stem/stromal cell secretome for lung regeneration: the long way through "pharmaceuticalization" for the best formulation, J. Control Release 309 (2019) 11–24.
6 J. Behnke, S. Kremer, T. Shahzad, C.M. Chao, E. Bo¨ttcher-Friebertsh¨auser, R. E. Morty, et al., MSC based therapies-new perspectives for the injured lung, J. Clin. Med. 9 (2020).
7 D.C. Oniciu, T. Hashiguchi, Y. Shibazaki, C.L. Bisgaier, Gemcabene downregulates inflammatory, lipid-altering and cell-signaling genes in the STAMTM model of NASH, PloS one 13 (2018), e0194568.
8 W.X. Chen, J. Zhou, S.S. Zhou, Y.D. Zhang, T.Y. Ji, X.L. Zhang, et al., Microvesicles derived from human Wharton's jelly mesenchymal stem cells enhance autophagy and ameliorate acute lung injury via delivery of miR-100, Stem Cell Res. Ther. 11 (2020) 113.
9 S. Dahbour, F. Jamali, D. Alhattab, A. Al-Radaideh, O. Ababneh, N. Al-Ryalat, et al., Mesenchymal stem cells and conditioned media in the treatment of multiple sclerosis patients: clinical, ophthalmological and radiological assessments of safety and efficacy, CNS Neurosci. Ther. 23 (2017) 866–874.
10 F. Dalouchi, R. Falak, M. Bakhshesh, Z. Sharifiaghdam, Y. Azizi, N. Aboutaleb, Human amniotic membrane mesenchymal stem cell-conditioned medium reduces inflammatory factors and fibrosis in ovalbumin-induced asthma in mice, Exp. Physiol. 106 (2021) 544–554.
11 A. De Becker, I.V. Riet, Homing and migration of mesenchymal stromal cells: how to improve the efficacy of cell therapy? World J Stem Cells 8 (2016) 73–87.
12 Y. Enomoto, S. Matsushima, K. Shibata, Y. Aoshima, H. Yagi, S. Meguro, et al., LTBP2 is secreted from lung myofibroblasts and is a potential biomarker for idiopathic pulmonary fibrosis, Clin. Sci. (Lond.) 132 (2018) 1565–1580.
13 R.G. Felix, A.L.C. Bovolato, O.S. Cotrim, P.D.S. Le˜ao, S.S. Batah, M.A. Golim, et al., Adipose-derived stem cells and adipose-derived stem cell-conditioned medium modulate in situ imbalance between collagen I- and collagen V-mediated IL-17 immune response recovering bleomycin pulmonary fibrosis, Histol. Histopathol. 35 (2020) 289–301.
14 E. Filidou, V. Valatas, I. Drygiannakis, K. Arvanitidis, S. Vradelis, G. Kouklakis, et al., Cytokine receptor profiling in human colonic subepithelial myofibroblasts: a differential effect of Th polarization associated cytokines in intestinal fibrosis, Inflamm.Bowel Dis. 24 (10) (2018) 2224–2241.
15 E.J. Freireich, E.A. Gehan, D.P. Rall, L.H. Schmidt, H.E. Skipper, Quantitative comparison of toxicity of anticancer agents in mouse, rat, hamster, dog, monkey, and man, Cancer Chemother. Rep. 50 (1966) 219–244.
16 L.E. Gosselin, J.E. Williams, M. Deering, D. Brazeau, S. Koury, D.A. Martinez, Localization and early time course of TGF-beta 1 mRNA expression in dystrophic muscle, Muscle Nerve 30 (2004) 645–653.
17 H. Guo, Y. Wang, H. Cui, Y. Ouyang, T. Yang, C. Liu, et al., Copper induces spleen damage through modulation of oxidative stress, apoptosis, DNA damage, and inflammation, Biol. Trace Elem. Res. (2021), https://doi.org/10.1007/s12011- 021-02672-8. Online ahead of print.
18 C.R. Harrell, D. Miloradovic, R. Sadikot, C. Fellabaum, B.S. Markovic, D. Miloradovic, et al., Molecular and cellular mechanisms responsible for beneficial effects of mesenchymal stem cell-derived product "Exo-d-MAPPS" in attenuation of chronic airway inflammation, Anal Cell Pathol (Amst) 2020 (2020) 3153891.
19 C.K. How, Y. Chien, K.Y. Yang, H.C. Shih, C.C. Juan, Y.P. Yang, et al., Induced pluripotent stem cells mediate the release of interferon gamma-induced protein 10 and alleviate bleomycin-induced lung inflammation and fibrosis, Shock 39 (2013) 261–270.
20 A. Ioannidis, K. Arvanitidis, E. Filidou, V. Valatas, G. Stavrou, A. Michalopoulos, et al., The length of surgical skin incision in postoperative inflammatory reaction 22 (2018).
21 G. Izbicki, M. J. Segel, T.G. Christensen, M.W. Conner, R. Breuer, Time course of bleomycin-induced lung fibrosis, Int. J. Exp. Pathol. 83 (2002) 111–119.
22 J. Janockova, L. Slovinska, D. Harvanova, T. Spakova, J. Rosocha, New therapeutic approaches of mesenchymal stem cells-derived exosomes, J. Biomed. Sci. 28 (2021) 39.
23 A. Joseph, I. Baiju, I.A. Bhat, S. Pandey, M. Bharti, M. Verma, et al., Mesenchymal stem cell-conditioned media: a novel alternative of stem cell therapy for quality wound healing, J. Cell. Physiol. 235 (2020) 5555–5569.
24 H.Jung, H.H. Kim, D.H. Lee, Y.S. Hwang, H.C. Yang, J.C. Park, Transforming growth factor-beta 1 in adipose derived stem cells conditioned medium is a dominant paracrine mediator determines hyaluronic acid and collagen expression profile, Cytotechnology 63 (2011) 57–66.
25 Y.J. Kim, H.J. Ahn, S.H. Lee, M.H. Lee, K.S. Kang, Effects of conditioned media from human umbilical cord blood-derived mesenchymal stem cells in the skin immune response, Biomed. Pharmacother. 131 (2020), 110789.
26 T.E. King Jr., J.A. Tooze, M.I. Schwarz, K.R. Brown, R.M. Cherniack, Predicting survival in idiopathic pulmonary fibrosis: scoring system and survival model, Am. J. Respir. Crit. Care Med. 164 (2001) 1171–1181.
27 D.E. Lee, N. Ayoub, D.K. Agrawal, Mesenchymal stem cells and cutaneous wound healing: novel methods to increase cell delivery and therapeutic efficacy, Stem Cell Res. Ther. 7 (2016) 37.
28 F. Luppi, M. Kalluri, P. Faverio, M. Kreuter, G. Ferrara, Idiopathic pulmonary fibrosis beyond the lung: understanding disease mechanisms to improve diagnosis and management, Respir. Res. 22 (2021) 109.
29 X. Ma, J. Chen, J. Liu, B. Xu, X. Liang, X. Yang, et al., IL-8/CXCR2 mediates tropism of human bone marrow-derived mesenchymal stem cells toward CD133(+) /CD44(+) Colon cancer stem cells, J. Cell. Physiol. 236 (2021) 3114–3128.
30 R.P. Meier, R. Mahou, P. Morel, J. Meyer, E. Montanari, Y.D. Muller, et al., Microencapsulated human mesenchymal stem cells decrease liver fibrosis in mice, J. Hepatol. 62 (2015) 634–641.
31 A. Mohammadipoor, B. Antebi, A.I. Batchinsky, L.C. Cancio, Therapeutic potential of products derived from mesenchymal stem/stromal cells in pulmonary disease, Respir. Res. 19 (2018) 218.
32 A. Nabil, K. Uto, F. Zahran, R. Soliman, A.A. Hassan, M.M. Elshemy, et al., The potential safe antifibrotic effect of stem cell conditioned medium and nilotinib combined therapy by selective elimination of rat activated HSCs, Biomed. Res. Int. 2021 (2021) 6678913.
33 A.B. Nair, S. Jacob, A simple practice guide for dose conversion between animals and human, J. Basic Clin. Pharm. 7 (2016) 27–31.
34 OECD, Test No. 402: Acute Dermal Toxicity, 2017.
35 V. Paspaliaris, G. Kolios, Stem cells in osteoporosis: from biology to new therapeutic approaches, Stem Cells Int. 2019 (2019) 1730978.
36 Y. Pu, D. Cao, C. Xie, H. Pei, D. Li, M. Tang, et al., Anti-arthritis effect of a novel quinazoline derivative through inhibiting production of TNF-α mediated by TNF-α converting enzyme in murine collagen-induced arthritis model, Biochem. Biophys. Res. Commun. 462 (2015) 288–293.
37 G. Raghu, M. Remy-Jardin, J.L. Myers, L. Richeldi, C.J. Ryerson, D.J. Lederer, et al., Diagnosis of idiopathic pulmonary fibrosis. An official ATS/ERS/JRS/ALAT clinical practice guideline, Am. J. Respir. Crit. Care Med. 198 (2018) e44–e68.
38 L. Shao, Y. Zhang, W. Shi, L. Ma, T. Xu, P. Chang, et al., Mesenchymal stromal cells can repair radiation-induced pulmonary fibrosis via a DKK-1-mediated Wnt/β-catenin pathway, Cell Tissue Res. 384 (2021) 87–97.
39 Y. Shi, C. Nan, Z. Yan, L. Liu, J. Zhou, Z. Zhao, et al., Synaptic plasticity of human umbilical cord mesenchymal stem cell differentiating into neuron-like cells in vitro induced by edaravone, Stem Cells Int. 2018 (2018) 5304279.
40 N. Song, M. Scholtemeijer, K. Shah, Mesenchymal stem cell immunomodulation: mechanisms and therapeutic potential, Trends Pharmacol. Sci. 41 (2020) 653–664.
41 C. Tran, M.S. Damaser, Stem cells as drug delivery methods: application of stem cell secretome for regeneration, Adv. Drug Deliv. Rev. 82–83 (2015) 1–11.
42 A. Tzouvelekis, V. Paspaliaris, G. Koliakos, P. Ntolios, E. Bouros, A. Oikonomou, et al., A prospective, non-randomized, no placebo-controlled, phase Ib clinical trial to study the safety of the adipose derived stromal cells-stromal vascular fraction in idiopathic pulmonary fibrosis, J.Transl.Med. 11 (2013) 171.
43 S. Vakrou, M.A. Nana, I.A. Nanas, E. Nana-Leventaki, M. Bonios, C. Kapelios, et al., Safety and efficacy of global intracoronary administration of cardiosphere-derived cells or conditioned medium immediately after coronary reperfusion in rats, Hell. J. Cardiol. 61 (2020) 256–261.

44 C. Wang, H. Meng, X. Wang, C. Zhao, J . Peng, Y. Wang, Differentiation of bone marrow mesenchymal stem cells in osteoblasts and adipocytes and its role in treatment of osteoporosis, Med. Sci. Monit. 22 (2016) 226–233.

45 C. Xia, P. Chang, Y. Zhang, W. Shi, B. Liu, L. Ding, et al., Therapeutic effects of bone marrow-derived mesenchymal stem cells on radiation-induced lung injury, Oncol. Rep. 35 (2016) 731–738.

46 P. Xu, X. Yang, The efficacy and safety of mesenchymal stem cell transplantation for spinal cord injury patients: a meta-analysis and systematic review, Cell Transplant. 28 (2019) 36–46.

47 S. Yin, C. Ji, P. Wu, C. Jin, H. Qian, Human umbilical cord mesenchymal stem cells and exosomes: bioactive ways of tissue injury repair, Am. J . Transl. Res. 11 (2019) 1230–1240.

48 J . Zhao, L. Hu, J . Liu, N. Gong, L. Chen, The effects of cytokines in adipose stem cell-conditioned medium on the migration and proliferation of skin fibroblasts in vitro, Biomed. Res. Int. 2013 (2013), 578479.

49 T. Zhou, H.Y. Li, C. Liao, W. Lin, S. Lin, Clinical efficacy and safety of mesenchymal stem cells for systemic lupus erythematosus, Stem Cells Int. 2020 (2020) 6518508.